Spectral-domain Optical Coherence Tomography Imaging of Age-related Macular Degeneration

Carlos Alexandre de Amorim Garcia Filho, MD,[1] Philip J Rosenfeld, MD, PhD,[2] Zohar Yehoshua, MD, MHA[3] and Giovanni Gregori, PhD[3]

1. Postdoctoral Associate; 2. Professor of Ophthalmology; 3. Assistant Professor, Department of Ophthalmology, Bascom Palmer Eye Institute, University of Miami Miller School of Medicine

Abstract

Spectral-domain optical coherence tomography (SD-OCT) high-speed, high-resolution imaging of the macula has become an essential tool for evaluating dry and wet age-related macular degeneration (AMD). This high-speed, high-resolution imaging strategy, combined with new innovative algorithms, permits reproducible measurements of the anatomic changes associated with AMD, which include drusen, geographic atrophy (GA), and choroidal neovascularization (CNV). To visualize drusen and larger retinal pigment epithelial detachments, an algorithm was developed for Cirrus HD-OCT (Carl Zeiss Meditec, Dublin CA) to detect elevations in the retinal pigment epithelium (RPE). To visualize GA, an algorithm was developed to provide en face visualization of the macula, which easily identifies and measures areas where the RPE has been lost. To visualize CNV and the associated macular fluid, an algorithm was developed to measure the retinal thickness between the internal limiting membrane and the RPE. No other imaging modality is capable of qualitatively and quantitatively following patients at all stages of AMD, which makes SD-OCT the ideal instrument for following disease progression and the effect of therapies.

Keywords

Age-related macular degeneration, drusen, geographic atrophy, retinal pigment epithelium, retinal pigment epithelial detachment, choroidal neovascularization, spectral-domain optical coherence tomography

Disclosure: Carlos Alexandre de Amorim Garcia Filho, MD, Phillip J Rosenfeld, MD, PhD, and Zohar Yehoshua, MD, MHA, have received research support from Carl Zeiss Meditec, Inc. Giovanni Gregori, PhD, and the University of Miami co-own a patent that is licensed to Carl Zeiss Meditec, Inc. Phillip J Rosenfeld, MD, PhD, has received honoraria for lectures from Carl Zeiss Meditec, Inc.

Acknowledgment: OCT images in this article are from the Cirrus HD-OCT (Carl Zeiss Meditec, Dublin CA).

Received: August 2, 2011 **Accepted:** August 23, 2011 **Citation:** *US Opthalmic Review,* 2011;4(2):113–8 *DOI: 10.17925/USOR.2011.04.02.113*

Correspondence: Philip J Rosenfeld, MD, PhD, Bascom Palmer Eye Institute, 900 NW 17th Street, Miami, FL 33136. E: prosenfeld@med.miami.edu

Support: The publication of this article was funded by Carl Zeiss Meditec, Inc.

Age-related macular degeneration (AMD) is a common cause of irreversible vision loss among the elderly worldwide. It is estimated that approximately 30 % of adults older than 75 years have some sign of AMD and that approximately 10 % of these patients have advanced stages of the disease.[1–4] AMD can be classified in two forms: non-neovascular (dry) and neovascular (wet or exudative). The non-neovascular form accounts for 80–90 % of cases, while the neovascular form accounts for 10–20 % of cases, but the neovascular form is responsible for the majority of the cases with severe vision loss (80–90 %).[4]

Time-domain optical coherence tomography (OCT) is a non-contact optical technique that images the retina and the macular area.[5] Spectral-domain OCT (SD-OCT), also known as Fourier-domain or high-definition OCT, is a higher-speed, higher-resolution technique that permits even better visualization of the retina, in particular the photoreceptor and retinal pigment epithelium (RPE) layers, as well as changes associated with disease progression.[6] SD-OCT instruments acquire images at a speed of at least 20,000 A-scans per second, compared with 400 A-scans per second for time-domain OCT. The higher speed and higher resolution of SD-OCT imaging result in the ability to cover a much larger area of the macula in greater detail and, with the use of new algorithms, these data sets can be reconstructed into 3D images of the macula. These images permit visualization of the real retinal geometry that is less affected by eye movements. Different scan patterns can be used depending on the information desired.[7] For example, the high speed of SD-OCT permits the acquisition of scan patterns with a large number of lower density B-scans. Segmentation algorithms have been developed to extract quantitative information from these SD-OCT data sets, which includes the retinal thickness map, the OCT fundus image (OFI), and an RPE elevation map. The retinal thickness map is ideally suited to show the accumulation of fluid in the macula or the increased thickness in the macula resulting from traction, the OFI is ideally suited to show the boundaries of

Figure 1: Schematic Representation of the Spectral-domain Optical Coherence Tomography Algorithm

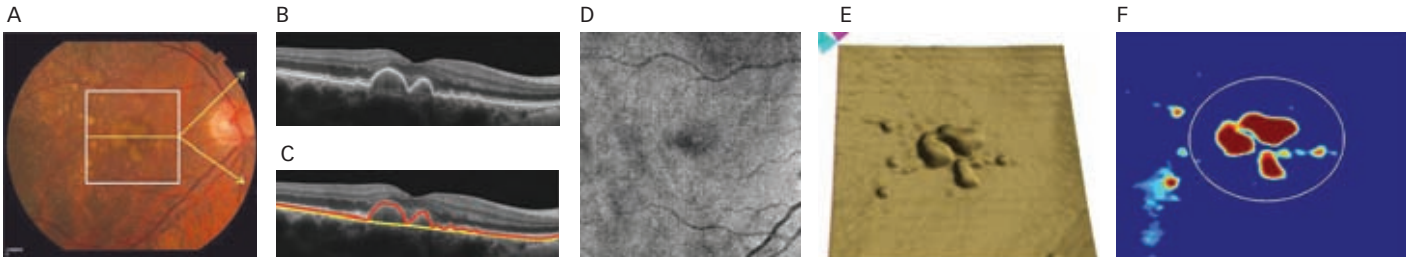

A: Color fundus image of a patient with drusen. A 6 x 6 mm white box was superimposed on the image to represent the scan area; B: B-scan from the spectral-domain optical coherence tomography data set that corresponds to the yellow line on the color fundus image; C: B-scan with a red line representing the retinal pigment epithelium (RPE) segmentation and a yellow line showing the RPE floor; D: En face image of the 6 x 6 mm scan pattern (optical coherence tomography fundus image); E: 3D RPE map delineating the drusen conformation; F: RPE elevation map.

Figure 2: Left Eye of a 67-year-old Woman with Drusen that Decreased Spontaneously over a Period of One Year

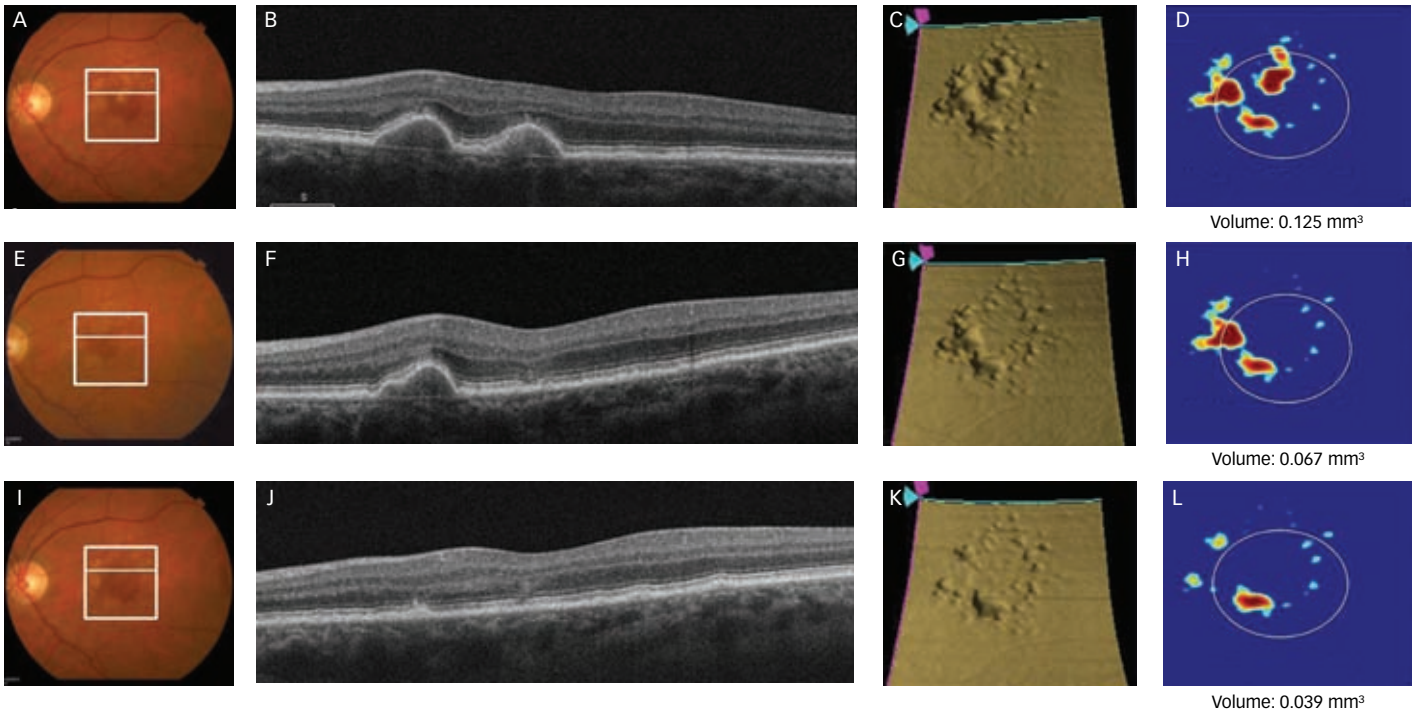

A–D: Color fundus images, horizontal B-scan, retinal pigment epithelium (RPE) map, and RPE elevation map of the baseline visit. Images are shown at six months (E–H) and one year (I–L) of follow-up. The drusen volume decreased from 0.125 mm^3 at baseline to 0.067 mm^3 at six months and 0.039 mm^3 at one year.

geographic atrophy (GA), and the RPE elevation map is ideally suited to show drusen and retinal pigment epithelial detachments (PEDs).[8–12] The ability to perform averaged B-scans increases image quality and can be used to evaluate subtle changes in retinal anatomy. The purpose of this article is to review the use of SD-OCT for the diagnosis, treatment, and follow-up of patients with AMD.

Spectral-domain Optical Coherence Tomography in Dry Age-related Macular Degeneration

Non-neovascular (dry) AMD is characterized by abnormalities of the RPE and the basement membrane between the RPE and choriocapillaris. Deposits develop under the RPE and within Bruch's membrane. These deposits can be seen ophthalmoscopically as drusen, which can be scattered throughout the macula and posterior pole. Deposits can also be seen on top of the RPE and these are known as subretinal drusenoid deposits. Increased pigment clumping at the level of the RPE is another characteristic sign of AMD, followed by focal atrophy of the RPE. These abnormalities may be asymptomatic or accompanied by compromised vision, and are considered to be the precursors of GA and choroidal neovascularization (CNV).[13–15]

Drusen

Drusen appear clinically as focal, white-yellow excrescences deep to the retina. They vary in number, size, shape, and distribution. Several grading strategies have been developed to image drusen using color fundus photography.[16,17] Although color fundus photography is useful for assessing the appearance of drusen, these images only provide 2D area information on the geometry of the drusen and cannot be used to measure quantitative properties such as drusen volume. SD-OCT can provide a 3D geometric assessment of drusen.

The high-definition averaged B-scans are useful for assessing the ultrastructure of drusen and to examine adjacent retinal layers that can be compromised by the disease process. Schuman et al. used

Figure 3: Right Eye of a 72-year-old Man with Drusen that Increased in Volume during 16 Months of Follow-up

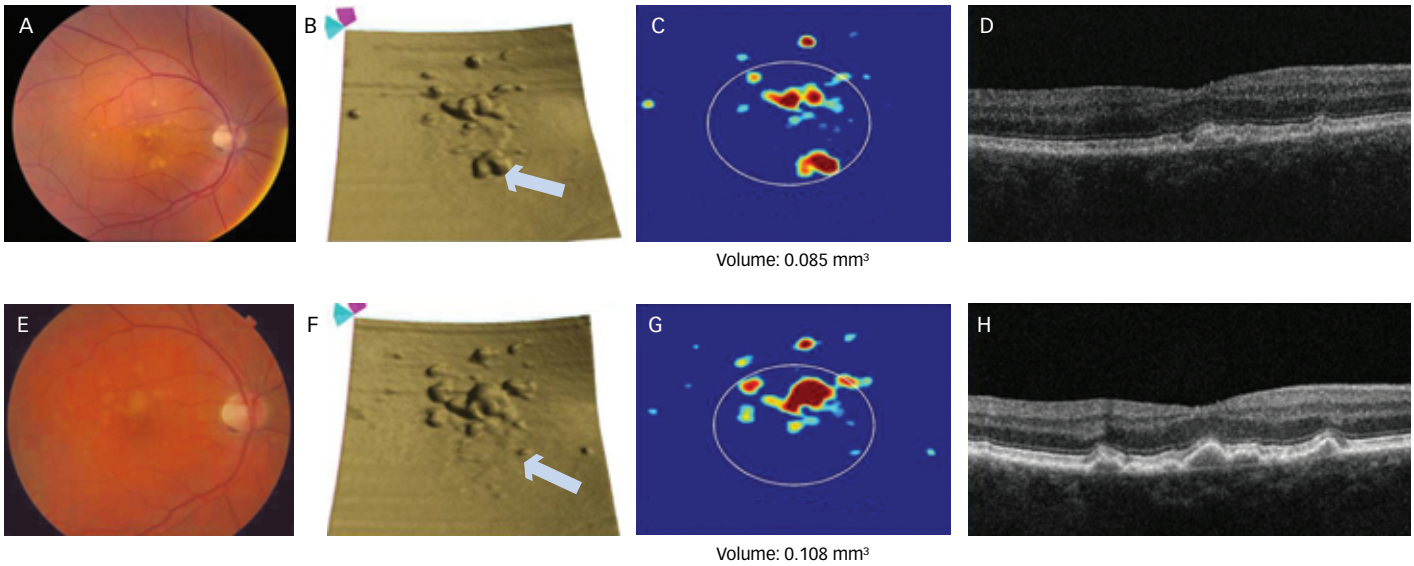

A–D: Color fundus images, retinal pigment epithelium (RPE) map, RPE elevation map, and horizontal B-scan from the baseline visit; E–H: Color fundus images after 16 months of follow-up. The volume within a 3 mm circle increased from 0.085 to 0.108 mm³ (C and G). Some areas of drusen disappeared during the follow-up period (B and F, white arrow) while the total drusen volume increased over time.

SD-OCT to examine the retinal layers overlying drusen. A thinning in the photoreceptor layer was observed in 97 % of the cases, with an average photoreceptor layer thickness reduced by 27 % compared with age-matched control eyes. The inner retinal layers remained unchanged. They observed a correlation between the decrease of photoreceptor layer thickness and the height of drusen. These findings suggest a degenerative process, with photoreceptor loss leading to visual impairment.[18]

The acquisition of raster scans comprising a large number of lower-density B-scans, combined with the use of segmentation algorithms, results in the ability to generate maps of the internal limiting membrane and the RPE, which provides information on the RPE geometry and therefore a unique perspective of drusen. A novel algorithm developed to identify RPE elevations, such as drusen, has been shown to be highly reproducible in the quantification of drusen area and volume.[11] This new algorithm creates a drusen map from a scan pattern of 40,000 uniformly spaced A-scans organized as 200 A-scans in each B-scan and 200 horizontal B-scans, covering an area of 6 x 6 mm centered in the fovea. The algorithm uses the actual RPE geometry and compares this RPE segmentation map with a virtual map of the RPE free of deformations (RPE floor). Using these two maps, the algorithm creates an elevation map, which permits reproducible measurements of drusen area and volume. Using this algorithm, Yehoshua et al. reported the natural history of drusen in AMD. Based on their findings, drusen were shown to undergo three different growth patterns. In most eyes, drusen were found to increase in volume and area. Drusen could also remain stable or they could dramatically decrease over time. When these drusen decreased, they could develop into GA or neovascular AMD, or they could decrease resulting in no residual defect in the macula.[19]

An example of the segmentation algorithm used to measure drusen is shown in *Figure 1*. In this figure, the 6 x 6 mm scan area (white box) was superimposed on a color fundus image of a macula containing drusen (see *Figure 1A*). A representative B-scan is shown with the boundaries of the actual RPE segmentation and the interpolated RPE floor identified in red and yellow, respectively (see *Figures 1B* and *1C*). In *Figure 1D*, the OFI is shown, which represents the summation of the reflected light from each A-scan when viewed en face. This topic will be discussed later in this article. A 3D RPE segmentation map is shown along with the RPE elevation map, which represents the difference between the actual RPE and the RPE floor for each B-scan in the data set, and this map is used to generate the area and volume of the drusen (see *Figures 1E* and *1F*).

Figures 2 and *3* represent the clinical use of SD-OCT when observing patients with dry AMD. *Figure 2* shows an example of an eye with significant regression of drusen as demonstrated using the algorithm. The color fundus image, a representative B-scan over the drusen, the RPE segmentation map, and the RPE elevation map with a 3 mm circle at baseline (see *Figures 2A–2D*), at six months (see *Figures 2E–2H*), and at one year (see *Figures 2I–2L*) of follow-up, respectively, are shown. The drusen area and volume decreased over time as shown most convincingly in the RPE segmentation and elevation maps. Drusen volume decreased from 0.125 mm³ at baseline to 0.067 mm³ at six months and to 0.039 mm³ at one year of follow-up.

Figure 3 shows an example of an eye with increasing drusen volume and area over 16 months. The volume within the 3 mm circle increases from 0.085 to 0.108 mm³. It is interesting to note that some areas of drusen disappear during the follow-up interval (*Figures 3B* and *3F*, white arrow) while the total drusen volume increases over time. This example demonstrates that drusen are dynamic.

Geographic Atrophy

The formation of GA impairs visual function, impacts the quality of life, and may result in blindness.[20] GA is seen clinically as one or more well-demarcated areas of hypopigmentation or depigmentation due to

Figure 4: 78-year-old Man with Geographic Atrophy

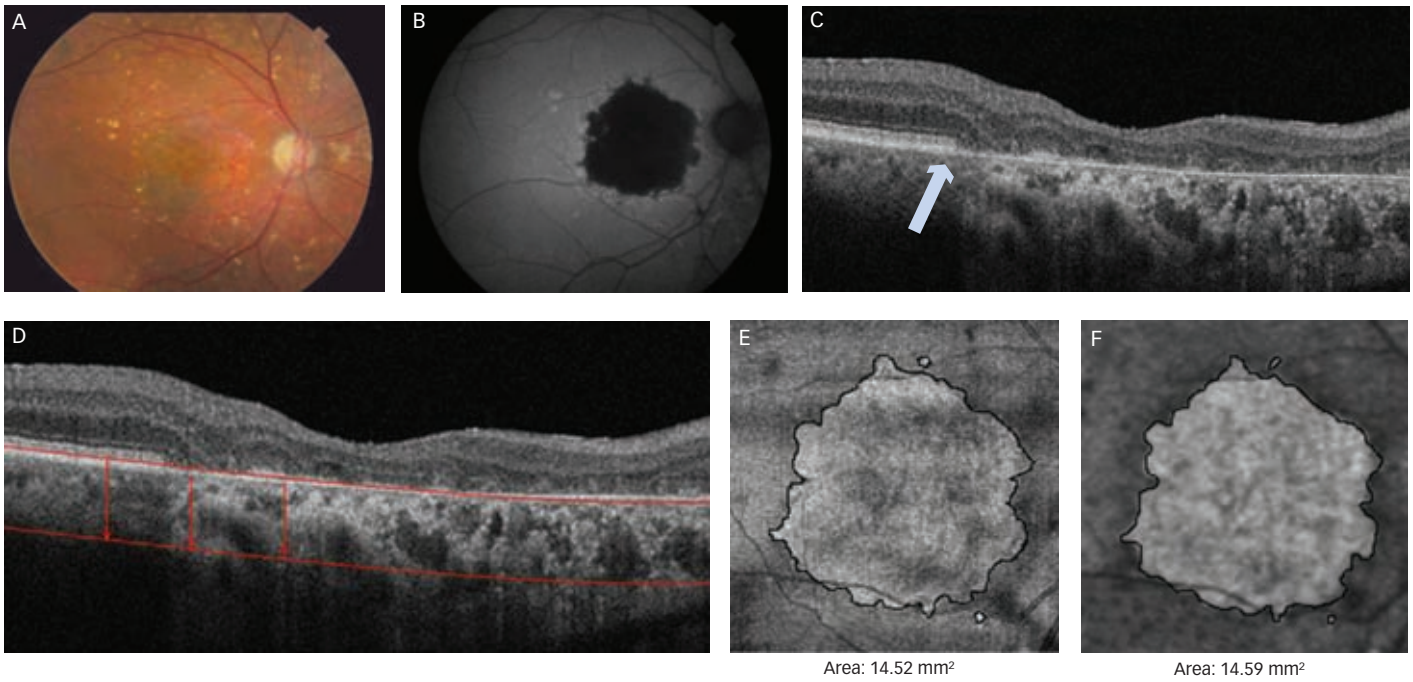

A: Color fundus images; B: Fundus autofluorescence (FAF) images. Observe the difficulty in identifying the entire lesion in the color images compared with the FAF images; C: Horizontal B-scan of the macula with increased choroidal light penetration in areas where the retinal pigment epithelium (RPE) is absent. The white arrow shows the transition between the areas where the RPE is present and absent; D: B-scan with red lines representing the sub-RPE layers used to compose the enhanced optical coherence tomography (OCT) fundus image; E: OCT fundus image; F: Enhanced OCT fundus image. The boundaries of the lesion were manually outlined.

Figure 5: Right Eye of a 76-year-old Woman with Wet Age-related Macular Degeneration

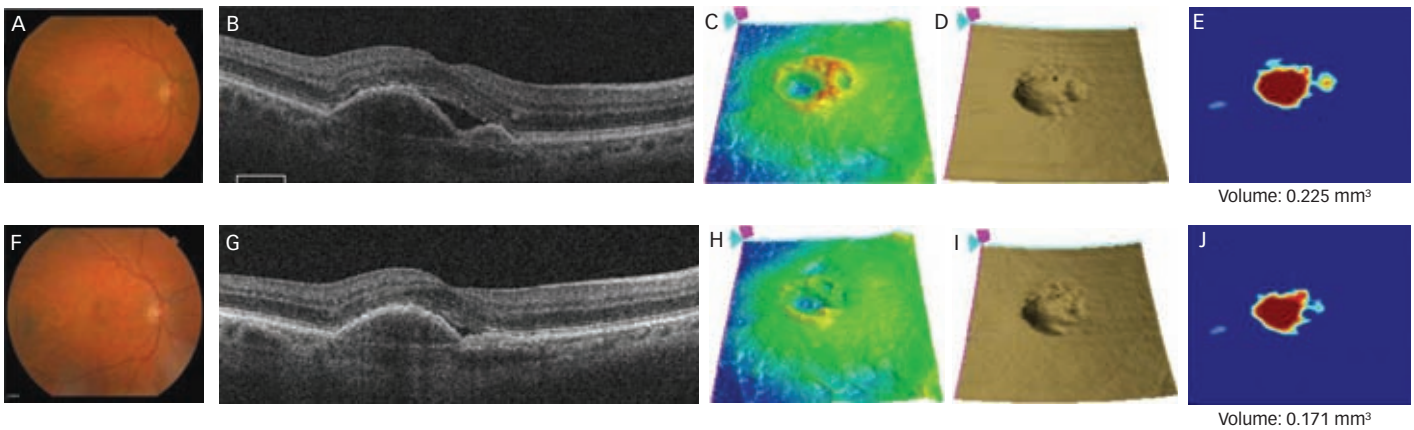

A: Color fundus images; B: Horizontal B-scan showing a pigment epithelial detachment (PED) and the presence of subretinal fluid; C: Retinal thickness map with areas of increased retinal thickness (red and yellow); D: Retinal pigment epithelium (RPE) segmentation map with a PED; E: RPE elevation map with quantization of the PED volume; F–J: Post-treatment images following the use of an intravitreal vascular endothelial growth factor (VEGF) inhibitor. The subretinal fluid on the B-scan (G) decreases, and the retinal thickness map (H) shows a corresponding decrease in thickness. The PED decreases as observed qualitatively on the RPE segmentation map (I) and the PED volume decreases as observed quantitatively on the RPE elevation map (J).

the absence or severe attenuation of the underlying RPE. The larger, deeper choroidal vessels are more readily visualized through the atrophic patches, which also lack photoreceptors and choriocapillaris. The natural history of GA has been described as a progressive condition that evolves through stages with loss of vision occurring over years.[8,21,22] The initial size and configuration of the atrophy appear to influence its progression rate. Average linear rates of growth of 140–200 µm/year from the GA margin have been reported, and the area of GA may enlarge by up to 3 mm² or more annually.[20,21,23–25] Multiple imaging modalities have been used to document and quantify the area of GA. Historically, color fundus photography was used to image GA; however, the use of color photos can be challenging due to the reported difficulty in detecting and accurately delineating GA.[21,26,27] Other imaging modalities, such as fluorescein angiography (FA), fundus autofluorescence (FAF), and SD-OCT are now used to evaluate and quantify GA. Although these imaging modalities provide different information, none has been shown to be superior to another.

SD-OCT was shown to be a useful tool for imaging and measuring GA.[8,9,28] A wide spectrum of morphologic alterations can be observed when

evaluating eyes with GA using high-definition B-scans. The loss of the RPE and photoreceptors is easily observed in these B-scans. Bearelly et al. reported that photoreceptor loss occurred most frequently in a bridging fashion across the margin of GA.[28]

GA is currently imaged using SD-OCT by using the OFI, which represents a virtual fundus image resulting from the en face summation of the reflected light from each A-scan. This en face OFI identifies GA as a bright area, due to the increased penetration of light into the choroid where atrophy has occurred in the macula. The absence of the RPE and choriocapillaris are responsible for this increased penetration of light associated with GA.[8,9] The OFI was shown to correlate well with the GA seen on clinical examination, color fundus imaging, and autofluorescence imaging.[10,28,29]

More recently, a newer algorithm developed by Carl Zeiss Meditec, Inc., provides an enhanced OFI, which is the summation of the reflected light from beneath the RPE. In addition, this new algorithm automatically measures the area of GA. A study comparing the measurements of GA area with the OFI and the enhanced OFI showed excellent correlation between the different modalities (Pearson correlation 0.999) and a good correlation between the automated algorithm and the manual grading (Pearson correlation 0.795) (Yehoshua Z et al. Personal communication).

Figure 4 shows an eye with GA secondary to AMD. *Figures 4A* and *4B* show the color fundus image and FAF image of the right eye. The entire area of GA is difficult to visualize using the color fundus image, but more easily seen using FAF. The SD-OCT B-scan demonstrates the increased light penetration into the choroid in the area where the RPE is absent (see *Figure 4C*). At the border of GA, where there is a transition between intact and atrophic RPE, there is a marked difference in light penetration into the choroid (arrow). This transition in the penetration of light is responsible for creating the border of GA seen with the en face imaging. Within the GA, the area of RPE atrophy appears brighter on the en face image because of the increased penetration of light into the choroid. The summation of the reflected light from the sub-RPE layers is used to compose the enhanced OFI (see *Figure 4D*, area between red lines). A good correlation can be observed between the OFI (see *Figure 4E*) and the enhanced OFI (see *Figure 4F*). The manual measurements of the GA areas were 14.52 and 14.59 mm^2 for the OFI and the enhanced OFI, respectively.

The advantage of the enhanced OFI is that the lesions usually appear brighter than in the OFI, which facilitates identification of the lesion's boundary. Another advantage is the fact that the OFI represents the light reflected from all the retinal layers, and the presence of other macular pathologies may interfere with the identification of GA.

Spectral-domain Optical Coherence Tomography in Wet Age-related Macular Degeneration

The neovascular (wet) form of AMD is responsible for the majority of the cases with severe vision loss. It is characterized by the growth of abnormal vessels in the macular region induced by the overproduction of vascular endothelial growth factor (VEGF). These vessels may arise from the choroidal circulation and penetrate Bruch's membrane to form a fibrovascular tissue external to the RPE, or they may arise primarily from the retinal circulation. In either case, the presence of VEGF and abnormal vessels leads to anatomic changes in the retina and choroid with the accumulation of fluid in the subretinal space, within the retina, or under the RPE.

Since the advent of drugs that inhibit VEGF, the ideal strategy for following eyes with wet AMD has been to use OCT to determine whether the treatment is effective in resolving the macular fluid. The macular fluid can be identified by examining the B-scans and by reviewing the retinal thickness maps, which calculate the retinal thickness between the internal limiting membrane and the RPE. The effect of anti-VEGF therapy can then be assessed based on the qualitative appearance of the B-scans and the qualitative, as well as quantitative, changes in the retinal thickness maps. In addition, the same algorithm used to measure drusen can also be used to measure retinal pigment epithelial detachments (PEDs) since both involve the elevation of the RPE. This algorithm will measure both the area and volume of a PED. Penha et al. showed excellent reproducibility when measuring the area and volume of PEDs in patients with wet AMD.[12] Moreover, Penha et al. have shown that changes in these quantitative measurements of PEDs may be useful in making retreatment decisions (unpublished data).

Figure 5 shows the case of a 76-year-old woman with wet AMD before treatment (upper row) and after treatment (lower row) with a single injection of an anti-VEGF drug. In *Figure 5A* the color fundus image shows the lesion and in *Figure 5B* the B-scan shows the macular fluid and a PED. The retinal thickness map (see *Figure 5C*) shows the area where the retinal thickness is increased (yellow and red areas). The RPE segmentation map shown in *Figure 5D* provides a 3D contour of the PED. *Figure 5E* shows the RPE elevation map with a PED volume measurement of 0.225 mm^3. After an intravitreal injection of an anti-VEGF drug, the amount of subretinal fluid decreases, as shown in the color fundus image (see *Figure 5F*), the B-scan (see *Figure 5G*), and the retinal thickness map (see *Figure 5H*). The PED volume decreases, as shown in *Figures 5I* and *5J*. The PED volume decreased to 0.171 mm^3 after treatment. This case demonstrates the usefulness of SD-OCT in the management of patients with wet AMD.

Summary

The recent advances in OCT technology, combined with the development of new algorithms capable of identifying RPE elevations and GA, provide quantitative tools for following patients with both wet and dry AMD. This imaging approach provides one-stop shopping for clinicians interested in managing patients with AMD. The advantage of SD-OCT over other imaging modalities for AMD is that the same scan pattern can be used to image the progression from drusen to GA and CNV. No other imaging modality is able to quantitatively assess all forms of AMD, so now clinicians can reliably follow the normal disease progression of their patients and their response to therapy. Although SD-OCT has changed the way we image AMD, the future of OCT holds even more promise with the use of longer-wavelength light sources for deeper choroidal penetration, faster scan times, and higher image resolution. ■

1. Bressler NM, Bressler SB, Congdon NG, et al., Potential public health impact of age-related disease study results: AREDS report no. 11, *Arch Ophthalmol*, 2003;121(11):1621–4.
2. Klein R, Peto T, Bird A, et al., The epidemiology of age-related macular degeneration, *Am J Ophthalmol*, 2004;137(3):486–95.
3. Congdon N, O'Colmain B, Klaver CC, et al., Causes and prevalence of visual impairment among adults in United States, *Arch Ophthalmol*, 2004;122(4):477–85.
4. Friedman DS, O'Colmain BJ, Muñoz B, et al., Prevalence of age-related macular degeneration in the United States, *Arch Ophthalmol*, 2004;122(4):564–72.
5. Huang D, Swanson EA, Lin CP, et al., Optical coherence tomography, *Science*, 1991;254:1178–81.
6. Drexler W, Sattmann H, Hermann B, et al., Enhanced visualization of macular pathology with the use of ultrahigh-resolution optical coherence tomography, *Arch Ophthalmol*, 2003;121:695–706.
7. Khanifar AA, Koreishi AF, Izatt JA, Toth CA, Drusen ultrastructure imaging with spectral domain optical coherence tomography in age-related macular degeneration, *Ophthalmology*, 2008;115:1883–90.
8. Jiao S, Knighton R, Huang X, et al., Simultaneous acquisition of sectional and fundus ophthalmic images with spectral-domain optical coherence tomography, *Opt Express*, 2005;13:444–52.
9. Wojtkowski M, Srinivasan V, Fujimoto JG, et al., Three-dimensional retinal imaging with high-speed ultrahigh resolution optical coherence tomography, *Ophthalmology*, 2005;112:1734–46.
10. Lujan BJ, Wang F, Gregori G, et al., Calibration of fundus images using spectral domain optical coherence tomography, *Ophthalmic Surg Lasers Imaging*, 2008;39(4 Suppl.):S15–20.
11. Gregori G, Wang F, Rosenfeld PJ, et al., Spectral domain optical coherence tomography imaging of drusen in non-exudative age-related macular degeneration, *Ophthalmology*, 2011;118(7):1373–9.
12. Penha FM, Rosenfeld PJ, Gregori G, et al., Quantitative imaging of retinal pigment epithelial detachments using spectral domain optical coherence tomography, *Am J Ophthalmol*, in press.
13. Hirvela H, Luukinen H, Läärä E, et al., Risk factors of age-related maculopathy in a population 70 years of age or older, *Ophthalmology*, 1996;103(6):871–7.
14. Klein R, Klein BE, Franke T, The relationship of cardiovascular disease and its risk factors to age-related maculopathy. The Beaver Dam Eye Study, *Ophthalmology*, 1993;100(3):406–14.
15. Vingerling JR, Hofman A, Grobbee DE, et al., Age-related macular degeneration and smoking. The Rotterdam Study, *Arch Ophthalmol*, 1996;114(10):1193–6.
16. Bartlett H, Eperjesi F, Use of fundus imaging in quantification of age-related macular change, *Surv Ophthalmol*, 2007;52(6):655–71.
17. Seddon JM, Sharma S, Adelman RA, Evaluation of the clinical age-related maculopathy staging system, *Ophthalmology*, 2006;113:260–6.
18. Schuman SG, Koreishi AF, Farsiu S, et al., Photoreceptor layer thinning over drusen in eyes with age-related macular degeneration imaged in vivo with spectral-domain optical coherence tomography, *Ophthalmology*, 2009;116:488–96.
19. Yehoshua Z, Wang F, Rosenfeld PJ, et al., Natural history of drusen morphology in age-related macular degeneration using spectral domain optical coherence tomography, *Ophthalmology*, 2011; [Epub ahead of print].
20. Sunness JS, The natural history of geographic atrophy, the advanced atrophic form of age-related macular degeneration, *Mol Vis*, 1999;5:25.
21. Sunness JS, Bressler NM, Tian Y, et al., Measuring geographic atrophy in advanced age-related macular degeneration, *Invest Ophthalmol Vis Sci*, 1999;40:1761–9.
22. Sarks JP, Sarks SH, Killingsworth MC, Evolution of geographic atrophy of the retinal pigment epithelium, *Eye (Lond)*, 1988;2:552–77.
23. Sunness JS, Gonzalez-Baron J, Applegate CA, et al., Enlargement of atrophy and visual acuity loss in the geographic atrophy form of age-related macular degeneration, *Ophthalmology*, 1999;106(9):1768–79.
24. Yehoshua Z, Rosenfeld PJ, Gregori G, et al., Progression of Geographic atrophy in age related macular degeneration imaged with spectral domain optical coherence tomography, *Ophthalmology*, 2011;118(4):679–86.
25. Holz FG, Bindewald-Wittich A, Fleckestein M, et al., Progression of geographic atrophy and impact of fundus autofluorescence patterns in age-related macular degeneration, *Am J Ophthalmol*, 2007;143(3):463–72.
26. Davis MD, Gangnon RE, Lee LY, et al., The Age-Related Eye Disease Study severity scale for age-related macular degeneration: AREDS Report No. 17, *Arch Ophthalmol*, 2005;123:1484–98.
27. Sunness JS, Ziegler MD, Applegate CA, Issues in quantifying atrophic macular disease using retinal autofluorescence, *Retina*, 2006;26:666–72.
28. Bearelly S, Chau FY, Koreishi A, et al., Spectral domain optical coherence tomography imaging of geographic atrophy margins, *Ophthalmology*, 2009;116:1762–9.
29. Drexler W, Fujimoto JG, State-of-the-art retinal optical coherence tomography, *Prog Retin Eye Res*, 2008;27:45–88